Cell Reports, Volume *33*

Supplemental Information

Epigenomic Reprogramming toward Mesenchymal-Epithelial Transition in Ovarian-Cancer-Associated Mesenchymal Stem Cells Drives Metastasis

Huihui Fan, Huda I. Atiya, Yeh Wang, Thomas R. Pisanic, Tza-Huei Wang, Ie-Ming Shih, Kelly K. Foy, Leonard Frisbie, Ronald J. Buckanovich, Alison A. Chomiak, Rochelle L. Tiedemann, Scott B. Rothbart, Chelsea Chandler, Hui Shen, and Lan G. Coffman

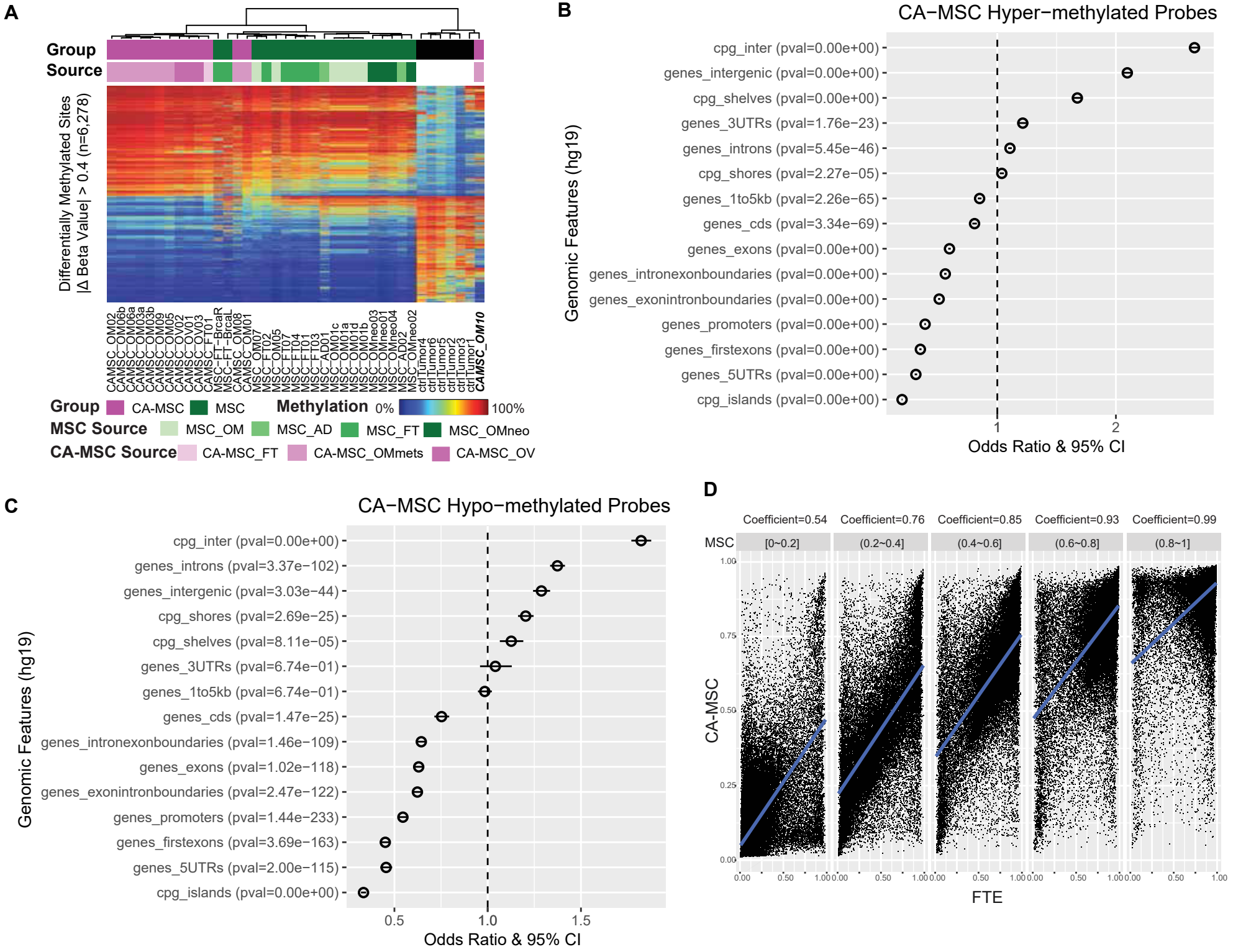
A
Group
Source
Differentially Methylated Sites
|Δ Beta Value| > 0.4 (n=6,278)
CAMSC_OM02
CAMSC_OM06b
CAMSC_OM06a
CAMSC_OM03a
CAMSC_OM03b
CAMSC_OM09
CAMSC_OM05
CAMSC_OV02
CAMSC_OV01
CAMSC_OV03
CAMSC_FT01
MSC_FT_BrcaR
MSC_FT_BrcaL
CAMSC_OM08
CAMSC_OM01
MSC_OM07
MSC_FT02
MSC_OM05
MSC_FT07
MSC_FT04
MSC_FT01
MSC_FT03
MSC_AD01
MSC_OM01c
MSC_OM01a
MSC_OM01d
MSC_OM01b
MSC_OMneo03
MSC_OMneo01
MSC_OMneo04
MSC_AD02
MSC_OMneo02
ctrlTumor4
ctrlTumor6
ctrlTumor5
ctrlTumor2
ctrlTumor3
ctrlTumor1
CAMSC_OM10
Group CA-MSC MSC
Methylation 0% 100%
MSC Source MSC_OM MSC_AD MSC_FT MSC_OMneo
CA-MSC Source CA-MSC_FT CA-MSC_OMmets CA-MSC_OV
B
CA−MSC Hyper−methylated Probes
Genomic Features (hg19)
cpg_inter (pval=0.00e+00)
genes_intergenic (pval=0.00e+00)
cpg_shelves (pval=0.00e+00)
genes_3UTRs (pval=1.76e−23)
genes_introns (pval=5.45e−46)
cpg_shores (pval=2.27e−05)
genes_1to5kb (pval=2.26e−65)
genes_cds (pval=3.34e−69)
genes_exons (pval=0.00e+00)
genes_intronexonboundaries (pval=0.00e+00)
genes_exonintronboundaries (pval=0.00e+00)
genes_promoters (pval=0.00e+00)
genes_firstexons (pval=0.00e+00)
genes_5UTRs (pval=0.00e+00)
cpg_islands (pval=0.00e+00)
1
2
Odds Ratio & 95% CI
C
CA−MSC Hypo−methylated Probes
Genomic Features (hg19)
cpg_inter (pval=0.00e+00)
genes_introns (pval=3.37e−102)
genes_intergenic (pval=3.03e−44)
cpg_shores (pval=2.69e−25)
cpg_shelves (pval=8.11e−05)
genes_3UTRs (pval=6.74e−01)
genes_1to5kb (pval=6.74e−01)
genes_cds (pval=1.47e−25)
genes_intronexonboundaries (pval=1.46e−109)
genes_exons (pval=1.02e−118)
genes_exonintronboundaries (pval=2.47e−122)
genes_promoters (pval=1.44e−233)
genes_firstexons (pval=3.69e−163)
genes_5UTRs (pval=2.00e−115)
cpg_islands (pval=0.00e+00)
0.5
1.0
1.5
Odds Ratio & 95% CI
D
Coefficient=0.54
Coefficient=0.76
Coefficient=0.85
Coefficient=0.93
Coefficient=0.99
MSC
[0~0.2]
(0.2~0.4]
(0.4~0.6]
(0.6~0.8]
(0.8~1]
CA-MSC
1.00
0.75
0.50
0.25
0.00
0.00
0.50
1.00
FTE

Figure S1. Additional DNA methylation differences in CA-MSCs vs MSCs, Related to Figure 1.

A. DNA methylation heatmap of top differentially methylated loci (FDR<0.05, and absolute group beta value difference > 0.4) between tumor samples and CA-MSCs. Probes are plotted as rows, with samples plotted as columns. Sample group of tumor, normal MSC, and CA-MSC is plotted as column annotation, together with sample isolation source if samples are normal MSCs or CA-MSCs. A blue-to-red gradient indicates a beta value of 0-1 (DNA methylation level of 0% to 100%). Sample CA-MSC_OM10 with heavy epithelial contamination is highlighted. Isolation site abbreviations: FT, fallopian tube; AD, adipose; OM, omentum; OV, ovary; OMmets, metastasis from omentum.

B,C. Enrichment of CA-MSC hyper-methylated loci (B) and hypo-methylated loci (C) against different genomic features of CpG and genic annotations. CpG annotations include open sea (cpg_inter), CpG shores (cpg_shores), CpG shelves (cpg_shelves), CpG islands (cpg_islands). Genic annotations contain 1-5Kb upstream of the TSS (genes_1to5kb), the promoter (< 1Kb upstream of the TSS; genes_promoters), 5'UTR (genes_5UTRs), first exons (genes_firstexons), exons (genes_exons), introns (genes_introns), CDS (genes_cds), 3'UTR (genes_3UTRs), and intergenic regions (the intergenic regions exclude the previous list of annotations; genes_intergenic). Odds ratio and 95% confidence interval (CI) for each feature are shown. Significance level is labeled in parentheses.

D. Scatter plots showing DNA methylation beta values in CA-MSC (shared y axis) versus fallopian tube epithelium (FTE) samples (x axes), stratified by the methylation level in normal MSCs. Each dot represent one CpG, as measured by one DNA methylation probe. Linear regression lines are plotted in blue, with corresponding regression coefficient (aka. slope) indicated on top of each panel.

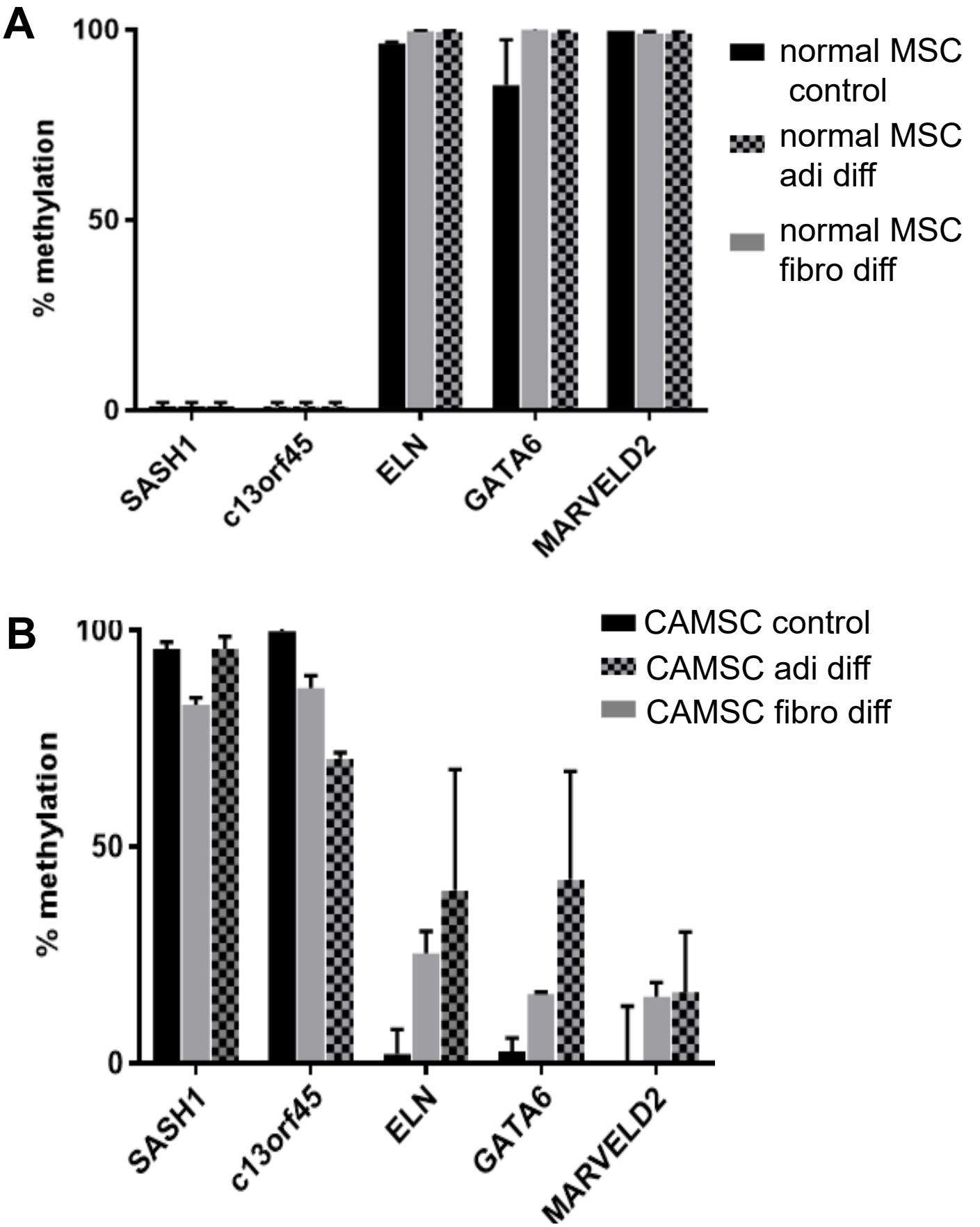
A
100
50
0
% methylation
SASH1
c13orf45
ELN
GATA6
MARVELD2
normal MSC control
normal MSC adi diff
normal MSC fibro diff
B
100
50
0
% methylation
SASH1
c13orf45
ELN
GATA6
MARVELD2
CAMSC control
CAMSC adi diff
CAMSC fibro diff

Figure S2. DNA methylation changes persists with MSC differentiation, Related to Figure 2.

A,B. DNA methylation levels at the five-locus panel for MSCs (A) and CA-MSCs (B) with adipose('adi') and fibroblast ('fibro') lineage differentiation. Y axis indicates % methylation as determined by MSP. Ttest between MSCs at each loci $p>0.05$. Mean & SEM of 3 independent samples are represented.

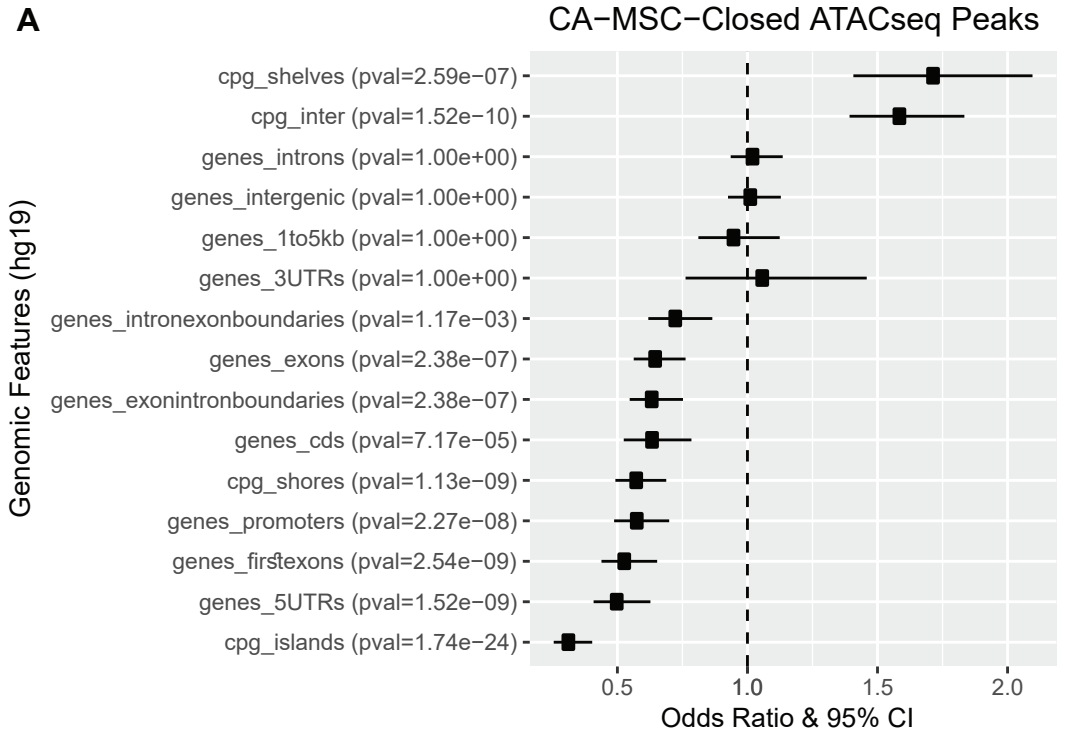
A
CA−MSC−Closed ATACseq Peaks
Genomic Features (hg19)
cpg_shelves (pval=2.59e−07)
cpg_inter (pval=1.52e−10)
genes_introns (pval=1.00e+00)
genes_intergenic (pval=1.00e+00)
genes_1to5kb (pval=1.00e+00)
genes_3UTRs (pval=1.00e+00)
genes_intronexonboundaries (pval=1.17e−03)
genes_exons (pval=2.38e−07)
genes_exonintronboundaries (pval=2.38e−07)
genes_cds (pval=7.17e−05)
cpg_shores (pval=1.13e−09)
genes_promoters (pval=2.27e−08)
genes_firstexons (pval=2.54e−09)
genes_5UTRs (pval=1.52e−09)
cpg_islands (pval=1.74e−24)
0.5
1.0
1.5
2.0
Odds Ratio & 95% CI

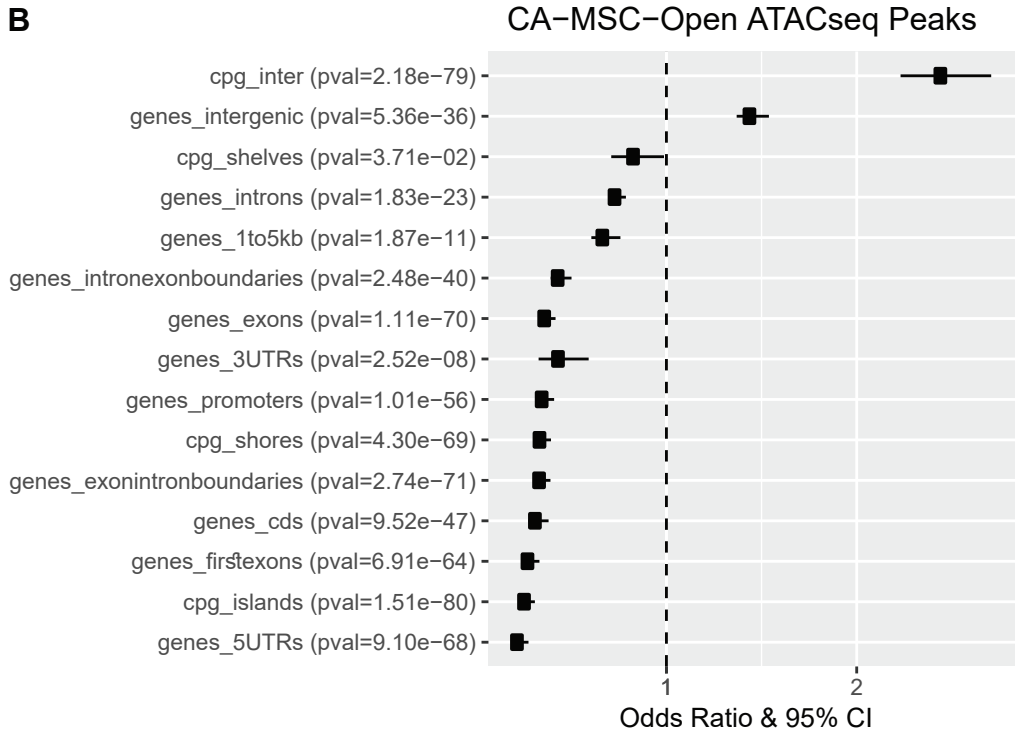
B
CA−MSC−Open ATACseq Peaks
cpg_inter (pval=2.18e−79)
genes_intergenic (pval=5.36e−36)
cpg_shelves (pval=3.71e−02)
genes_introns (pval=1.83e−23)
genes_1to5kb (pval=1.87e−11)
genes_intronexonboundaries (pval=2.48e−40)
genes_exons (pval=1.11e−70)
genes_3UTRs (pval=2.52e−08)
genes_promoters (pval=1.01e−56)
cpg_shores (pval=4.30e−69)
genes_exonintronboundaries (pval=2.74e−71)
genes_cds (pval=9.52e−47)
genes_firstexons (pval=6.91e−64)
cpg_islands (pval=1.51e−80)
genes_5UTRs (pval=9.10e−68)
1
2
Odds Ratio & 95% CI

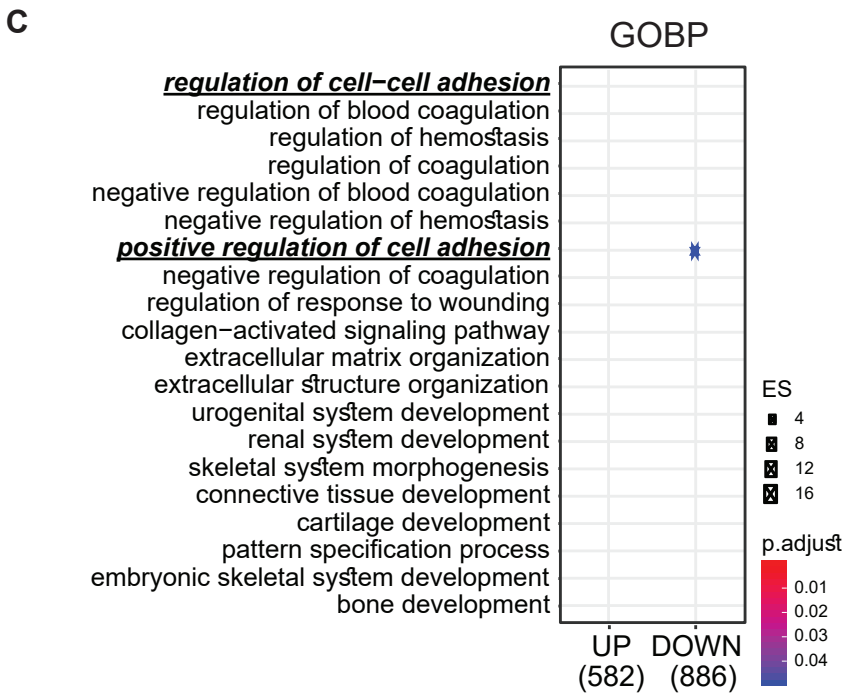
C
GOBP
regulation of cell−cell adhesion
regulation of blood coagulation
regulation of hemostasis
regulation of coagulation
negative regulation of blood coagulation
negative regulation of hemostasis
positive regulation of cell adhesion
negative regulation of coagulation
regulation of response to wounding
collagen−activated signaling pathway
extracellular matrix organization
extracellular structure organization
urogenital system development
renal system development
skeletal system morphogenesis
connective tissue development
cartilage development
pattern specification process
embryonic skeletal system development
bone development
UP (582)
DOWN (886)
ES
4
8
12
16
p.adjust
0.01
0.02
0.03
0.04

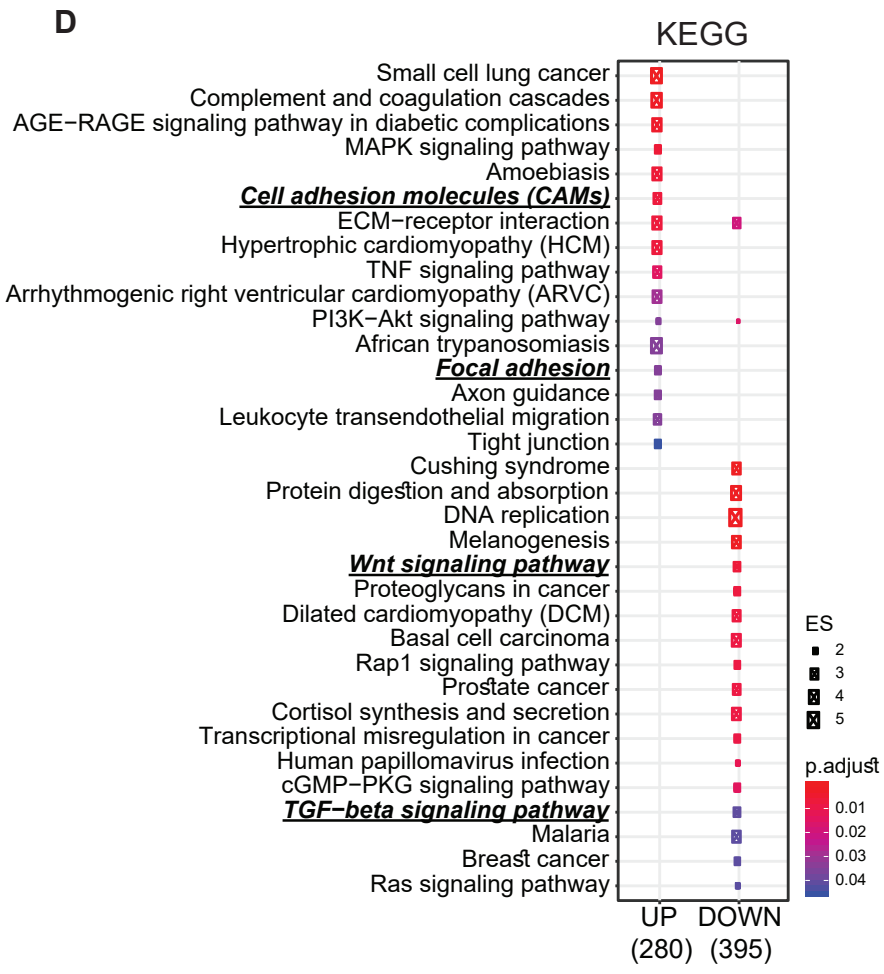
D
KEGG
Small cell lung cancer
Complement and coagulation cascades
AGE−RAGE signaling pathway in diabetic complications
MAPK signaling pathway
Amoebiasis
Cell adhesion molecules (CAMs)
ECM−receptor interaction
Hypertrophic cardiomyopathy (HCM)
TNF signaling pathway
Arrhythmogenic right ventricular cardiomyopathy (ARVC)
PI3K−Akt signaling pathway
African trypanosomiasis
Focal adhesion
Axon guidance
Leukocyte transendothelial migration
Tight junction
Cushing syndrome
Protein digestion and absorption
DNA replication
Melanogenesis
Wnt signaling pathway
Proteoglycans in cancer
Dilated cardiomyopathy (DCM)
Basal cell carcinoma
Rap1 signaling pathway
Prostate cancer
Cortisol synthesis and secretion
Transcriptional misregulation in cancer
Human papillomavirus infection
cGMP−PKG signaling pathway
TGF−beta signaling pathway
Malaria
Breast cancer
Ras signaling pathway
UP (280)
DOWN (395)
ES
2
3
4
5
p.adjust
0.01
0.02
0.03
0.04

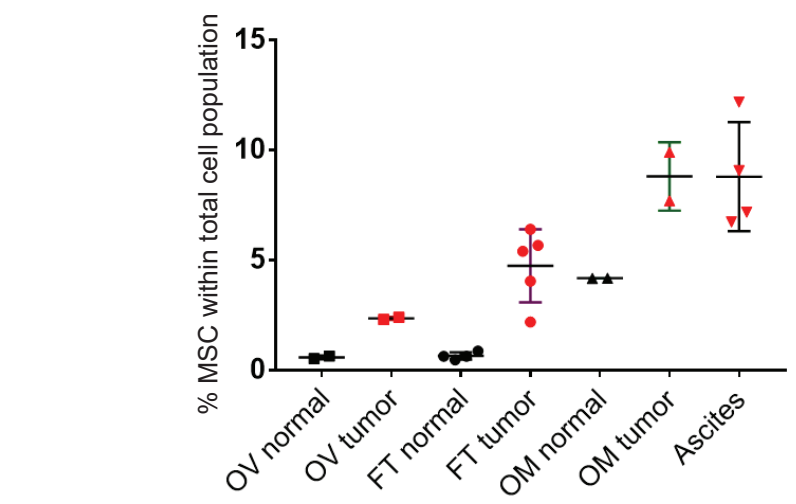
E
% MSC within total cell population
15
10
5
0
OV normal
OV tumor
FT normal
FT tumor
OM normal
OM tumor
Ascites

Figure S3. Additional ATAC-seq, pathway analysis and cellular abundance of CA-MSCs vs MSCs, Related to Figure 3 and 4.

A,B. Enrichment of CA-MSC closed (A) and open (B) ATAC-seq peaks against different genomic features of CpG and genic annotations defined as in Supp Figure S1B,C. Odds ratio and 95% confidence interval (CI) for each feature are shown. Significance level is labeled in parentheses.

C. Gene ontology (GO) enrichment analysis (biological concept of Biological Process; GOBP). The numbers of up- and down-regulated genes comparing CA-MSCs to MSCs are labeled underneath the plot. Each dot represents a GOBP term, with dot size indicating enrichment score (ES), and dot color representing significance level. Two cell adhesion related processes are highlighted for genes upregulated in CA-MSCs.

D. KEGG (Kyoto Encyclopedia of Genes and Genomes) pathway analysis. Two pathways relevant to cell adhesion are highlighted for upregulated genes, and two pathways relevant to EMT (epithelial-mesenchymal transition), the reverse process of MET, are highlighted for downregulated genes.

E. MSC quantification from benign and HGSC involved human tissues and ascites. MSCs quantified via flow cytometry (CD90, 73, 105+/CD45, 34, 14, 19- population) and represented as percentage of total viable cell population.

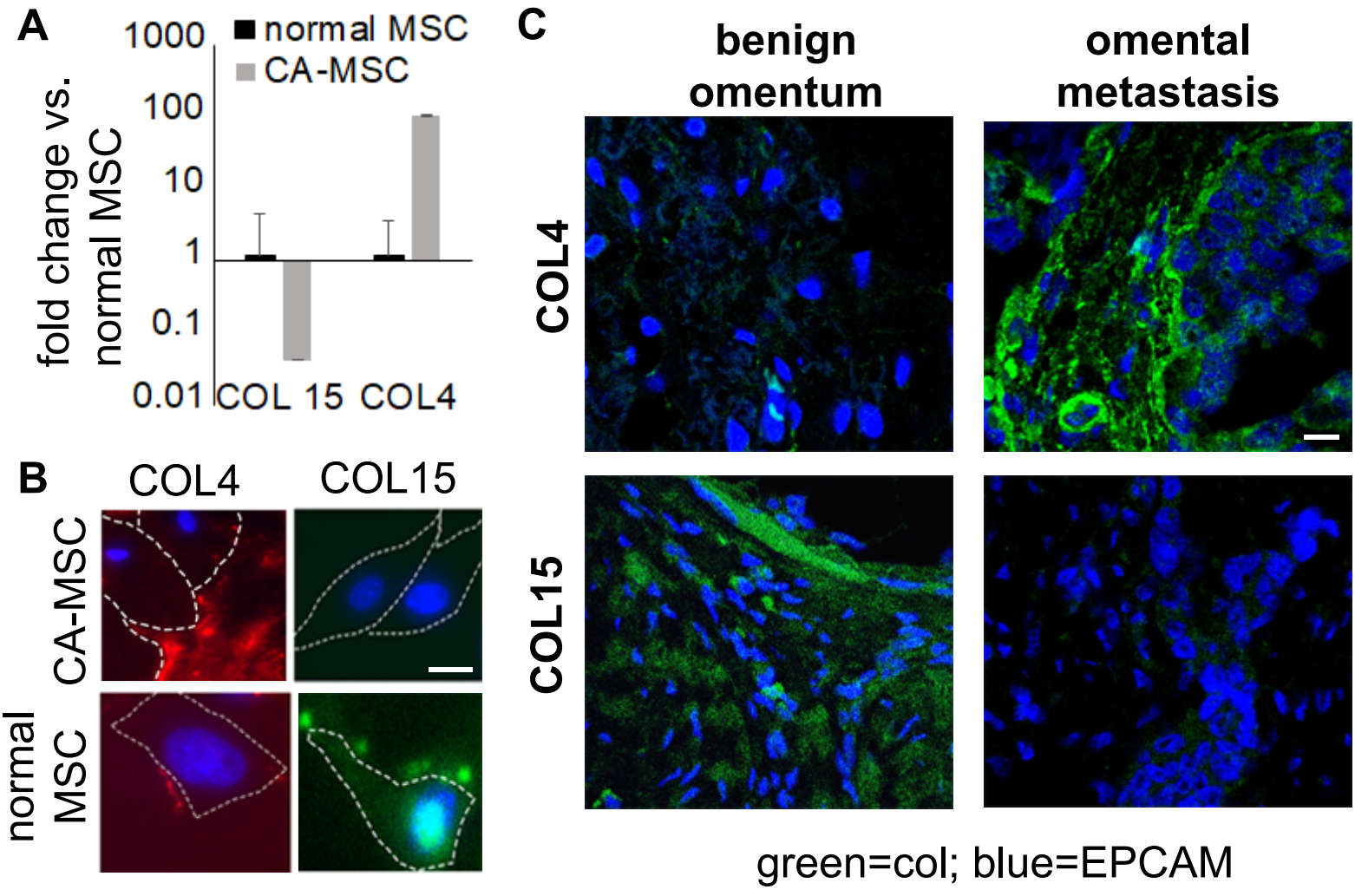
A
1000
100
10
1
0.1
0.01
normal MSC
CA-MSC
fold change vs. normal MSC
COL 15
COL4
B
COL4
COL15
CA-MSC
normal MSC
C
benign omentum
omental metastasis
COL4
COL15
green=col; blue=EPCAM

Figure S4. CA-MSCs have altered collagen secretion associated with increased metastasis, Related to Figure 3.

A. qRT-PCR of *COL15* and *COL4* expression in normal MSCs and CA-MSCs. Fold change compared to normal MSC is expressed. Results are the mean and SEM of 3 independent cell lines.
B. Immunofluorescence of COL4 (red) and COL15 (green) during adherent CA-MSC and normal MSC culture demonstrating increased CA-MSC secretion of COL4 and decreased secretion of COL15. Scale bar=10microns.
C. Immunofluorescence of COL4 and COL15 in benign omentum and omental HGSC metastasis demonstrating increased COL4 and decreased COL15 in omental metastasis. Scale bar=20microns

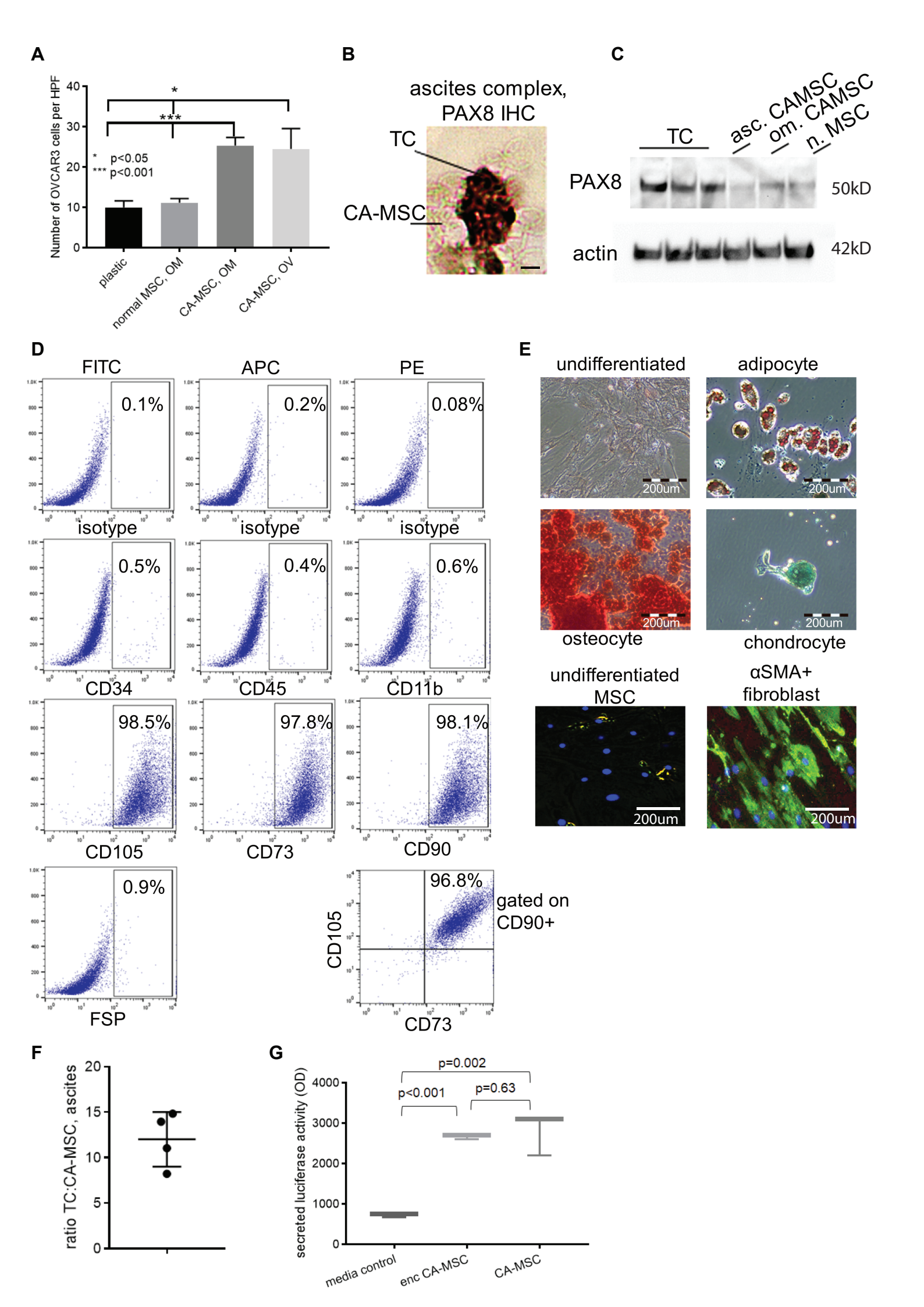
A
Number of OVCAR3 cells per HPF
40
30
20
10
0
*
***
* p<0.05
*** p<0.001
plastic
normal MSC, OM
CA-MSC, OM
CA-MSC, OV
B
ascites complex,
PAX8 IHC
TC
CA-MSC
C
TC
asc. CAMSC
om. CAMSC
n. MSC
PAX8
50kD
actin
42kD
D
FITC
APC
PE
0.1%
0.2%
0.08%
isotype
isotype
isotype
0.5%
0.4%
0.6%
CD34
CD45
CD11b
98.5%
97.8%
98.1%
CD105
CD73
CD90
0.9%
FSP
96.8%
CD105
CD73
gated on
CD90+
E
undifferentiated
adipocyte
200um
osteocyte
chondrocyte
undifferentiated
MSC
αSMA+
fibroblast
F
ratio TC:CA-MSC, ascites
20
15
10
5
0
G
secreted luciferase activity (OD)
4000
3000
2000
1000
0
p=0.002
p<0.001
p=0.63
media control
enc CA-MSC
CA-MSC

Figure S5. Additional tumor cell adhesion and CA-MSC verification, Related to Figure 4.

A. OVCAR3 binding to plastic, normal omentum (OM) MSCs, CA-MSCs derived from the OM and ovary (OV) demonstrates increased tumor cell adhesion to CA-MSCs. Results quantified by counting fluorescent tumor cells per high power field (HPF). Mean & SEM of 3 independent experiments is represented.

B. Immunohistochemistry of cytospin of CA-MSC:tumor cell complexes isolated from patient ascites demonstrating strong PAX8 expression in tumor cells and not CA-MSCs. Scale bar=20microns

C. PAX8 western blot of ovarian tumor cells and CA-MSCs isolated from ascites, omental metastasis and normal MSCs demonstrating CA-MSCs have minimal PAX8 expression which is similar to normal MSC levels and less than tumor cell levels.

D. CA-MSCs isolated from tissue and ascites complexes were verified to meet MSC differentiation and surface expression criteria. Representative flow cytometry plots characterizing MSCs based on CD105,73,90 positivity and CD34,45,11b negativity and negativity for the fibroblast marker, fibroblast surface protein (FSP). Last plot demonstrates the population triple positive for CD105, 73 and 90. Y axis represent side scatter unless otherwise noted.

E. Immunohistochemistry of undifferentiated and differentiated MSCs (adipocyte: oil red o; osteocyte: alizarin red; chondrocyte: alcian blue). Immunofluorescence of alpha-smooth muscle actin (αSMA) in undifferentiated and fibroblast differentiated MSCs demonstrating staining only after fibroblast directed differentiation.

F. Ratio of tumor cells to CA-MSCs in cellular complexes isolated from ascites. N=4 independent patients.

G. Secreted luciferase levels (OD measurement) in control media versus media from luciferase-secreting CA-MSCs in standard culture or alginate encapsulated CA-MSCs. Mean and SEM of 3 independent experiments.

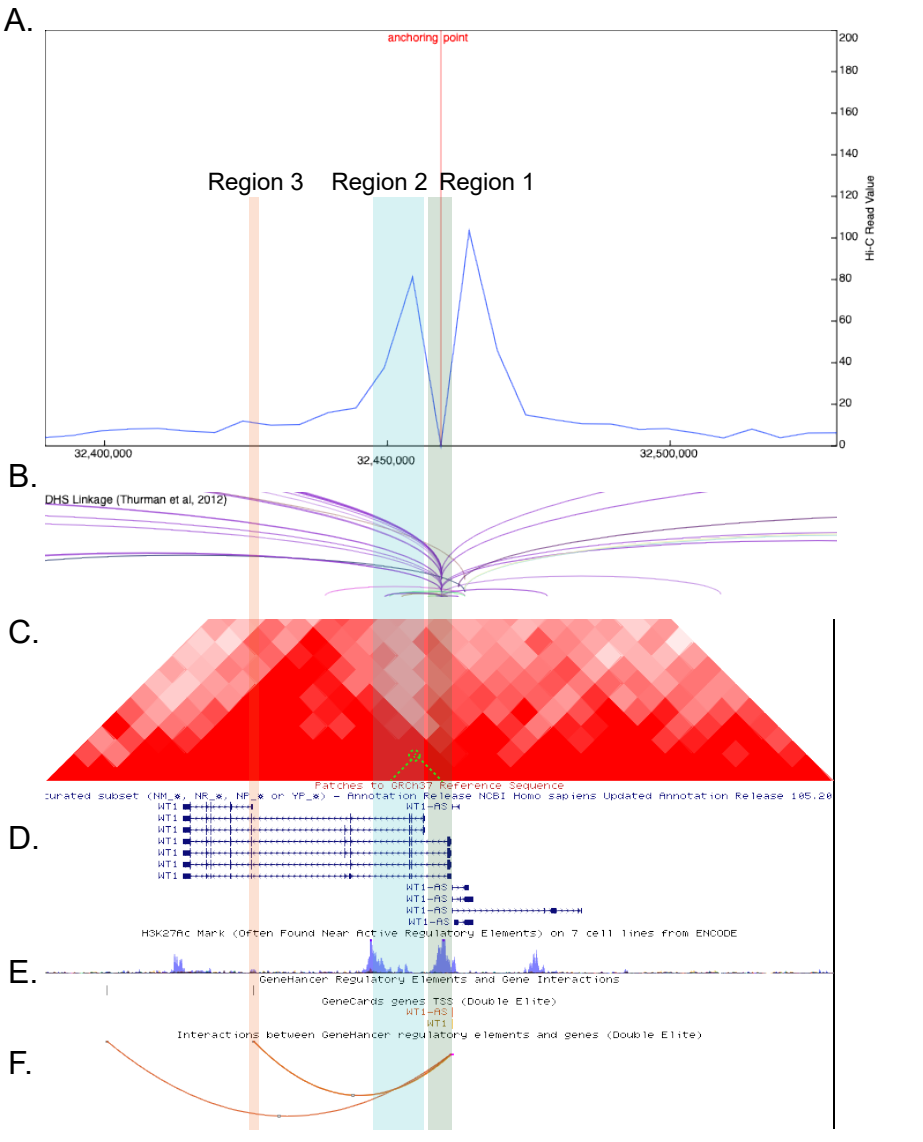
A.
anchoring point
Region 3
Region 2
Region 1
200
180
160
140
120
100
80
60
40
20
0
Hi-C Read Value
32,400,000
32,450,000
32,500,000
B.
DHS Linkage (Thurman et al, 2012)
C.
Patches to GRCh37 Reference Sequence
curated subset (NM_e, NR_e, NP_e or YP_e) - Annotation Release NCBI Homo sapiens Updated Annotation Release 105.20
WT1-AS
WT1
D.
H3K27Ac Mark (Often Found Near Active Regulatory Elements) on 7 cell lines from ENCODE
E.
GeneHancer Regulatory Elements and Gene Interactions
GeneCards genes TSS (Double Elite)
WT1-AS
WT1
Interactions between GeneHancer regulatory elements and genes (Double Elite)
F.

Figure S6. The 3D Genome Browser view in combination with the UCSC genomic view for gene *WT1* locus, Related to Figure 5.

A. Circular chromosomal conformation capture (4C) data in cell line K562 is plotted as a curve line (resolution is 5kb), where the center is the bait region (*WT1* TSS, covered by green box, Region 1) and a peak signal indicates there is a chromatin interaction event between the TSS and a potential distal regulatory region supported by HiC reads covering both regions (y-axis).

B-F. (B) DNase I-hypersensitive sites (DHS) linkage track and (C) UCSC tracks of HiC heatmap in K562, (D) gene track, (E) H3K27ac histone marks, and (F) enhancer, promoter, and regulatory interactions curated in GeneHancer database. Intense DHS interactions between the *WT1* promoter region (green box, Region 1) and the first potential enhancer within its gene body (cyan box, Region2) also supports the potential interactions. Dashed green lines and circle show consistency between the UCSC HiC heatmap track (resolution is 5kb) and the peak covered by cyan box (Region 2) from the 4C curve view. Orange box (Region 3) marks a second enhancer within gene *WT1*, which overlaps with known enhancer annotation, and interaction with the *WT1* promoter curated in the GeneHancer database.

A

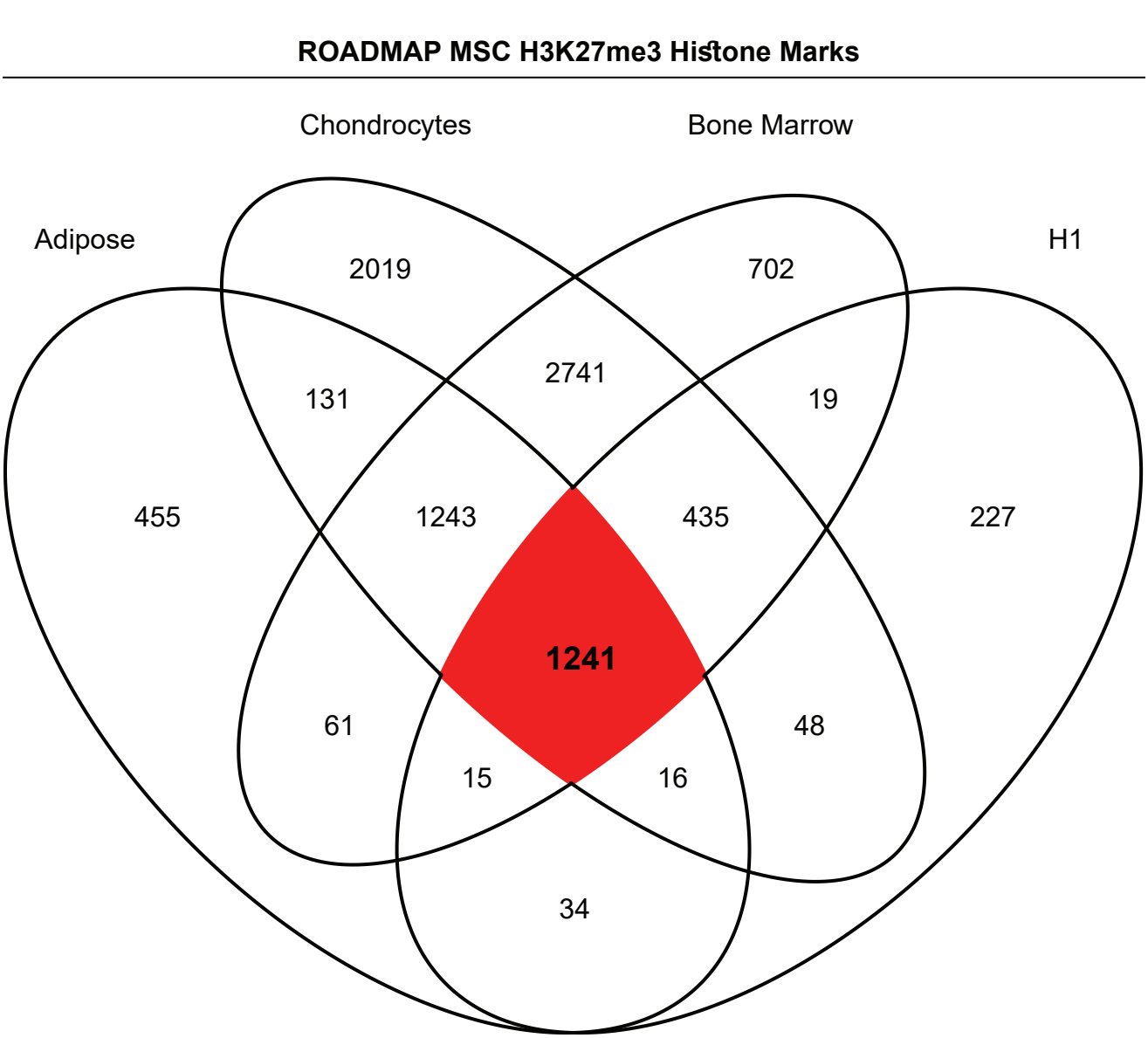
ROADMAP MSC H3K27me3 Histone Marks
Chondrocytes
Bone Marrow
Adipose
H1
2019
702
2741
131
19
455
1243
435
227
1241
61
48
15
16
34

B

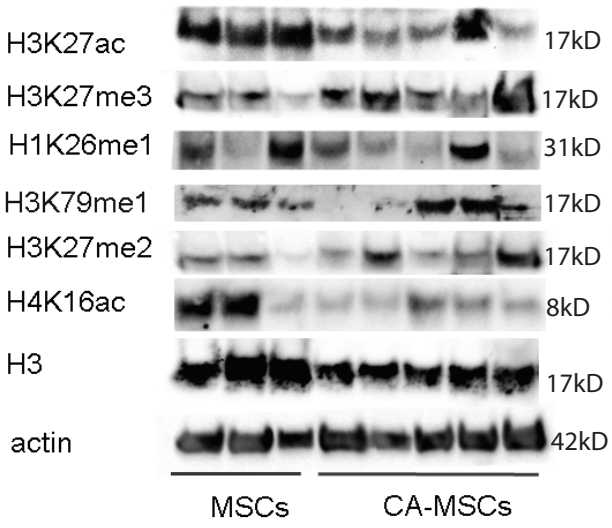
H3K27ac
H3K27me3
H1K26me1
H3K79me1
H3K27me2
H4K16ac
H3
actin
17kD
17kD
31kD
17kD
17kD
8kD
17kD
42kD
MSCs
CA-MSCs

C

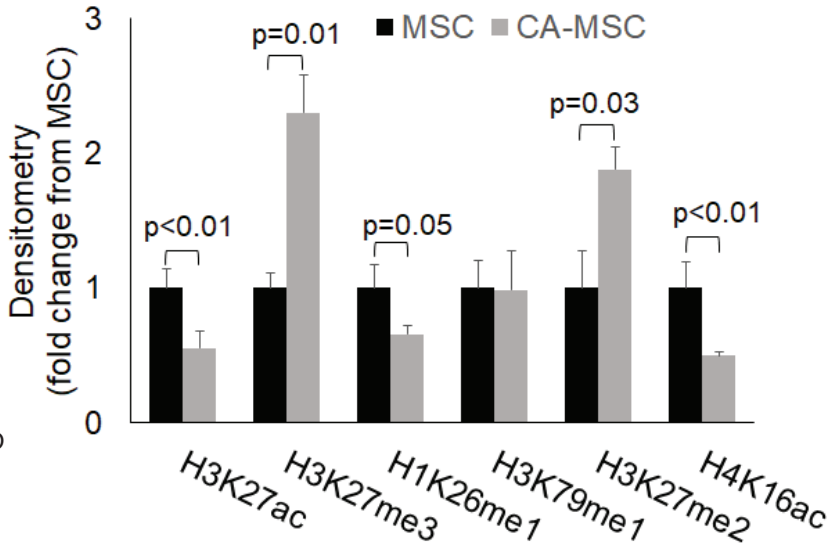
MSC
CA-MSC
Densitometry (fold change from MSC)
0
1
2
3
p<0.01
p=0.01
p=0.05
p=0.03
p<0.01
H3K27ac
H3K27me3
H1K26me1
H3K79me1
H3K27me2
H4K16ac

Figure S7. H3K27me3 peak overlap and verification of histone mass spectrometry, Related to Figure 6.

A. Venn diagram showing H3K27me3 peak overlaps among MSCs derived from different sources of adipose, chondrocytes, bone marrow, and H1 cell line. The common set of 1,241 narrow peak regions (as in red) is defined as the EZH2 targets, if they are located within their transcriptional regions plus 2 kb upstream flanking regions of their TSSs.

B. Western blot verification of differential histone modifications identified by mass spectrometry.

C. Densitometry quantification of western blot analysis of histone modifications normalized to actin (for H4K16ac and H1K26me1) and H3 (for H3 modifications), in 5 CA-MSCs compared to 3 MSCs. T- test p values between CA-MSC and normal MSC are labeled on top of the bar set for each histone type.

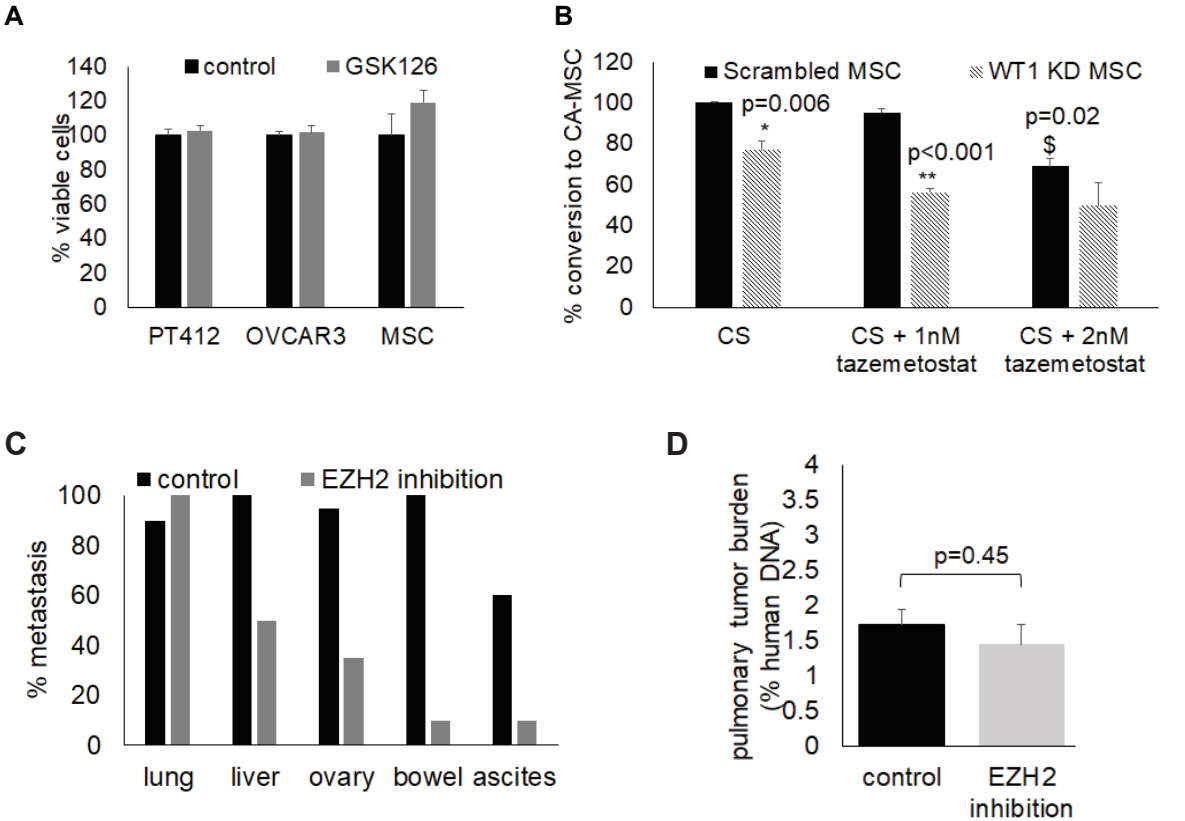
A
control
GSK126
% viable cells
140
120
100
80
60
40
20
0
PT412
OVCAR3
MSC
B
Scrambled MSC
WT1 KD MSC
% conversion to CA-MSC
120
100
80
60
40
20
0
p=0.006
*
p<0.001
**
p=0.02
$
CS
CS + 1nM tazemetostat
CS + 2nM tazemetostat
C
control
EZH2 inhibition
% metastasis
100
80
60
40
20
0
lung
liver
ovary
bowel
ascites
D
pulmonary tumor burden (% human DNA)
4
3.5
3
2.5
2
1.5
1
0.5
0
p=0.45
control
EZH2 inhibition

Figure S8. EZH2 inhibition does not impact tumor cell viability and additional EZH2 inhibitors similarly decrease CA-MSC formation, Related to Figure 4, 6 and STAR methods tissue harvesting.

A. Viability of tumor cells PT412 and OVCAR3 and normal MSCs after 5 days treatment with 20nM GSK126 compared to vehicle control.

B. Quantification of the percent of conversation to CA-MSC in WT1 KD MSCs or scrambled control after cancer stimulation (CS) with hypoxic direct cancer cell co-culture with and without a different EZH2 inhibitor, Tazemetostat. Values are normalized to scrambled control conversion based on CA-MSC classifier score. *, ** = comparison to treatment group scrambled control; $ = comparison to CS scrambled control without Tazemetostat. Mean & SEM of 3 independent experiments are shown.

C. EZH2 inhibition limits metastasis formation. Percentage of metastasis formation (y-axis) at different organ sites (x-axis) is shown between EZH2 inhibition and control group in a tail vein injection metastasis model.

D. Pulmonary tumor burden is shown between EZH2 inhibition and control group.

Table S1

SampleName	SampleID	PatientID	SampleGroup	SampleEPIC	Source	SourceCode
CAMSC_OM01	493_camsc	s493	CAMSC	201557520003_R03C01	CA-MSCs derived from the omental metastasis of patients with high grade serous ovarian cancer	CAMSC-OMmets
CAMSC_OM02	549_camsc	s549	CAMSC	201557520040_R03C01	CA-MSCs derived from the omental metastasis of patients with high grade serous ovarian cancer	CAMSC-OMmets
CAMSC_OM03a	CAMSC1	s0009	CAMSC	200516380137_R01C01	CA-MSCs derived from the omental metastasis of patients with high grade serous ovarian cancer	CAMSC-OMmets
CAMSC_OM03b	CAMSC2	s0009	CAMSC	200516380137_R02C01	CA-MSCs derived from the omental metastasis of patients with high grade serous ovarian cancer	CAMSC-OMmets
CAMSC_OM05	CAMSC3	s0003	CAMSC	200516380137_R03C01	CA-MSCs derived from the omental metastasis of patients with high grade serous ovarian cancer	CAMSC-OMmets
CAMSC_OM06a	CAMSC6	s0006	CAMSC	200516380137_R06C01	CA-MSCs derived from the omental metastasis of patients with high grade serous ovarian cancer	CAMSC-OMmets
CAMSC_OM06b	CAMSC7	s0006	CAMSC	200516380137_R07C01	CA-MSCs derived from the omental metastasis of patients with high grade serous ovarian cancer	CAMSC-OMmets
CAMSC_OM08	CAMSC8	s0008	CAMSC	200516380137_R08C01	CA-MSCs derived from the omental metastasis of patients with ovarian carcinosarcoma	CAMSC-OMmets
CAMSC_OM09	CAMSC9	s0009	CAMSC	200526210119_R01C01	CA-MSCs derived from the omental metastasis of patients with high grade serous ovarian cancer	CAMSC-OMmets
CAMSC_OM10	406_camsc	s406	CAMSC	201557520040_R02C01	CA-MSCs derived from the omental metastasis of patients with high grade serous ovarian cancer	CAMSC-OMmets
CAMSC_FT01	19-175 FT.camsc	s19-175	CAMSC	203020780110_R04C01	CAMSCs derived from fallopian tube invovled with high grade serous ovarian cancer	CAMSC-FT
CAMSC_OV01	19-90 ov.camsc	s19-90	CAMSC	203020780110_R05C01	CAMSCSs derived from ovary involved with high grade serous ovarian cancer	CAMSC-OV
CAMSC_OV02	19-95 ov.camsc	s19-95	CAMSC	203020780110_R06C01	CAMSCSs derived from ovary involved with high grade serous ovarian cancer	CAMSC-OV
CAMSC_OV03	19-263 ovcamsc	s19-263	CAMSC	203038250154_R06C01	CAMSCSs derived from ovary involved with ovarian cancer	CAMSC-OV
MSC_OMneo01	18-0030 neo n.om	s18-0030	MSC	203020780110_R08C01	MSCs derived from omentum that was initially involved with high grade serous ovarian cancer but had a complete pathologic response to neoadjuvant chemotherapy	MSC-OMneo
MSC_OMneo02	18-0054 neo n.om	s18-0054	MSC	203013220061_R01C01	MSCs derived from omentum that was initially involved with high grade serous ovarian cancer but had a complete pathologic response to neoadjuvant chemotherapy	MSC-OMneo
MSC_OMneo03	18-0048 neo n.om	s18-0048	MSC	203013220061_R02C01	MSCs derived from omentum that was initially involved with high grade serous ovarian cancer but had a complete pathologic response to neoadjuvant chemotherapy	MSC-OMneo
MSC_OMneo04	19-107 n.om (neo)	s19-107	MSC	203013220061_R03C01	MSCs derived from omentum that was never involved with cancer (stage II ovarian cancer) but patient had neoadjuvant chemotherapy	MSC-OMneo
MSC_FT01	19-120 n.FT	s19-120	MSC	203013220061_R04C01	MSCs derived from normal fallopian tube	MSC-FT
MSC_FT02	19-197 n.FT	s19-197	MSC	203013220061_R05C01	MSCs derived from normal fallopian tube	MSC-FT
MSC_FT03	19-128 n.FT	s19-128	MSC	203013220061_R06C01	MSCs derived from normal fallopian tube but with hydrosalpinx	MSC-FT
MSC_FT04	AL n.FT	s0007	MSC	203013220061_R07C01	MSCs derived from normal fallopian tube	MSC-FT
MSC-FT-BrcaL	19-257 LFT BRCA2	s19-257	MSC	203038250154_R02C01	MSCs derived from left fallopian tube with BRCA2 mutation	MSC-FT
MSC-FT-BrcaR	19-257 RFT BRCA2	s19-257	MSC	203038250154_R03C01	MSCs derived from right fallopian tube with BRCA2 mutation	MSC-FT
MSC_FT07	19-223 #2 nFT	s19-223	MSC	203038250154_R04C01	MSCs derived from normal fallopian tube	MSC-FT
MSC_AD01	amsc_1125	s1125	MSC	201557520040_R04C01	MSCs derived from adipose purchased through ATCC	MSC-AD
MSC_AD02	amsc_2118	s2118	MSC	201557520003_R05C01	MSCs derived from adipose purchased through ATCC	MSC-AD
MSC_OM01a	MSC1	s0001	MSC	200526210119_R02C01	MSCs derived from normal omental tissue undergoing surgery for benign indications	MSC-OM
MSC_OM01b	MSC2	s0001	MSC	200526210119_R03C01	MSCs derived from normal omental tissue undergoing surgery for benign indications	MSC-OM
MSC_OM01c	MSC5	s0001	MSC	200526210119_R06C01	MSCs derived from normal omental tissue undergoing surgery for benign indications	MSC-OM
MSC_OM01d	MSC6	s0001	MSC	200526210119_R07C01	MSCs derived from normal omental tissue undergoing surgery for benign indications	MSC-OM
MSC_OM05	18-691 n.om CC	s18-691	MSC	203013220061_R08C01	MSCs derived from normal omentum from patient with a stage II clear cell endometrial cancer	MSC-OM
MSC_OM05b	18-691 n.om CC	s18-691	MSC	203038250154_R01C01	MSCs derived from normal omentum from patient with a stage II clear cell endometrial cancer	MSC-OM
MSC_OM07	19-319 n.om	s19-319	MSC	203038250154_R05C01	MSCs derived from normal omentum	MSC-OM

Table S1. Sample list summary, Related to Figure 1 and STAR methods DNA methylation array